Monthly Notices
of the
ROYAL ASTRONOMICAL SOCIETY

Mon. Not. R. Astron. Soc. **403,** 1448–1456 (2010) doi:10.1111/j.1365-2966.2010.16209.x

Absolute parameters of young stars – II. V831 Centauri

E. Budding,[1,2,3]★ A. Erdem,[1] G. İnlek[4] and O. Demircan[1]

[1]*Physics Department, University of Canakkale, Terzioğlu Kampüsü, TR 17020 Canakkale, Turkey*
[2]*Carter National Observatory, Kelburn, Wellington, New Zealand*
[3]*Department of Physics and Astronomy, University of Canterbury, Christchurch 8140, New Zealand*
[4]*Department of Physics, University of Balikesir, Balikesir, Turkey*

Accepted 2009 December 12. Received 2009 December 11; in original form 2009 August 3

ABSTRACT

Literature photometry and new high-resolution spectroscopy of V831 Cen are presented and analysed. Light and radial velocity curve fittings confirm the central pair of this young multiple system to be close to contact. Absolute parameters are found as follows: $M_1 = 4.08 \pm 0.07\,\mathrm{M}_\odot$, $M_2 = 3.35 \pm 0.06\,\mathrm{M}_\odot$, $R_1 = 2.38 \pm 0.03\,\mathrm{R}_\odot$, $R_2 = 2.25 \pm 0.03\,\mathrm{R}_\odot$, $T_1 = 13\,000 \pm 300$ K, $T_2 = 11\,800 \pm 300$ K; distance of 110 ± 10 pc and age of $\sim 20 \pm 5$ Myr. Detailed examination of the spectrograms indicates the third component (V831 Cen B) to be an Ap star. The orbit of the third star about the close binary is analysed using historic astrometric measurements. This allows an estimate of the third star's mass to be about $2.5\,\mathrm{M}_\odot$, but this is sensitive to the adopted distance and inclination values. It is, however, confirmed by the measured radial velocity of the third star. To some extent, such analysis can also be applied to the fourth star (V831 Cen C). The derived properties can be checked against the system's membership of the Scorpius–Centaurus OB2 association.

Key words: methods: data analysis – binaries: close – stars: early-type – stars: individual: V831 Cen – Galaxy: stellar content.

1 INTRODUCTION

V831 Cen (=HD 114529, HIP 64425, HR 4975) is a bright ($V \approx 4.5 \sim 4.6$, $B - V \approx -0.08$, $U - B \approx -0.38$, $V - I \approx -0.07$ and $R - I \approx -0.09$) young B8V-type object, including a near-contact binary as well as some other stars. The sky location, a *Hipparcos* distance of 106 ± 16 pc and proper motions ($\mu_\alpha \cos\delta = -28.54$, $\mu_\delta = -17.46$ mas yr^{-1}) make the system a likely member of the Lower Centaurus Crux (LCC) concentration (Blaauw 1964) of the Scorpius–Centaurus OB2 (SCOB) association, within the Gould Belt's giant star formation region (Nitschelm 2004). The close binary V831 Cen (A = ab), lying relatively close to the disc ($l = 305\overset{\circ}{.}6$, $b = 2\overset{\circ}{.}9$), is the brighter component of the visual pair IDs 13060-5923 A-B (= See 170, separation of 183 mas, period of 27 yr), within a wider grouping of at least five stars (AB-C = I424, ABC-D = HDO 223; Worley 1978; Worley & Douglass 1996). The fairly scant attention given previously to this interesting system may be a consequence of its southerly declination $\sim -60^\circ$. The V magnitudes of the close visual double are estimated at 5.3 and 6.0 in the catalogue of Worley & Douglass (1996), but the combination of these magnitudes seems a little too faint: brighter values appeared in earlier sources.

★E-mail: budding@xtra.co.nz

The *Hipparcos* (ESA 1997) light curve has the published ephemeris

$$\mathrm{Min\,I} = 2448\,500.297 + 0.642\,52E. \quad (1)$$

The low amplitude (~15 per cent) variation, shown in Fig. 1, looks like that of a contact binary viewed with appreciable third light present, or at low inclination, so that the variation is characterized as 'ellipsoidal' (cf. SIMBAD).

Photometric variability of V831 Cen had been noted by Waelkens & Bartholdi (1982), who deduced, from their observed $U - B$ variations, that eclipses should be present. Given the shallowness of the minima and quasi-sinusoidal pattern of light variation, difficulties in finding a unique photometric model could be expected, though reasonable inferences can be made from combining various separate lines of evidence. In this connection, we may note that the original *Hipparcos* cataloguers could not find an acceptably precise single astrometric position for V831 Cen using only the satellite data, although it was known as a multiple star from early observations.

This paper continues with the southern binaries project of the Astrophysics Research Centre, 18th March University of Ćanakkale and the Carter National Observatory of New Zealand, utilizing eclipsing binary system analysis. Further background on this programme was given by Budding (2009) and Budding, İnlek & Demircan (2009, hereafter Paper I). In the following section, we discuss the photometry of V831 Cen ab, whose results are then

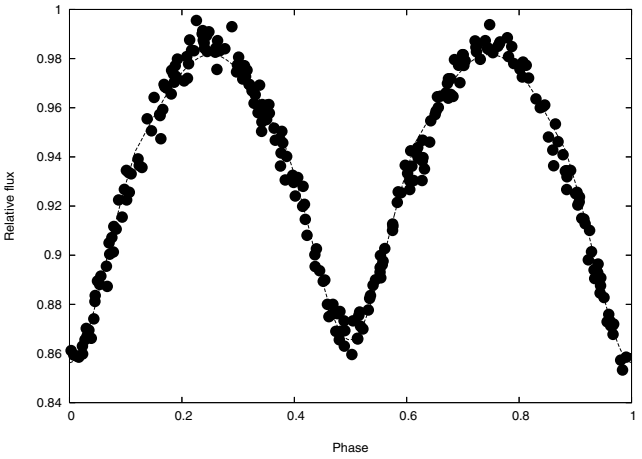

Figure 1. *Hipparcos V* photometry of V831 Cen and model fitting (see Section 2 for details).

combined with analysis of new spectroscopic material in Section 3 to refine knowledge of the absolute parameters of the components, concentrated on in Section 5. Before that, Section 4 discusses the astrometry of the multiple system. Section 6 summarizes the information derived within the context of the Galactic environment. The arrangement follows along similar lines to that of U Oph in Paper I.

2 PHOTOMETRY AND ANALYSIS

Light-curve fittings may start from preliminary estimates coming from inspection of the main features. In the case of V831 Cen, the reported $B - V$ (-0.08) and its apparent low level of variation are consistent with those of the B8V type reported in the SIMBAD data base. A primary temperature of $\sim$12 100 K can be provisionally assigned using the compilation of Budding & Demircan (2007). A trial main sequence (MS)-like model would then consist of two stars with total mass close to $7\,M_\odot$. The period (0.642 52 d), taken together with Kepler's third law and these masses, implies a separation of about $6.0\,R_\odot$. A normal main-sequence pair would have undistorted mean radii of about $2.4\,R_\odot$, implying an over-contact configuration for a close binary from Kopal's (1959) criterion for the relative radii ($r_1 + r_2 \sim 0.75$). Given the youth of this binary, however, its components may well have mean radii less than typical for the general field. This point, bearing on the age and structure of the stars, as well as other aspects of this preliminary picture, is open to more detailed analysis.

Starting from such estimates, the *Hipparcos V* light curve was well matched by the parameters given in Table 1. It should be noted that this ILOT-type curve fitting (cf. Paper I) corresponds to only a few free parameters, namely reference light (U) (normalized to unity in Table 1), component levels (L_1, L_3, with $L_2 = U - L_1 - L_3$) and inclination (i). A small shift to the zero-point of the *Hipparcos* phases ($\Delta\phi_0$) was also fitted. The other parameters come from the type-classification-based temperatures and expectation of near contact. The adopted mass ratio (0.82) comes from the spectroscopic data discussed in the next section, although the luminosity ratio L_2/L_1 supports a similar value. If we attempt to solve for more than a few parameters for such a quasi-sinusoidal light variation, the error matrix tends to degenerate and the solution becomes non-unique; even so, the two main stars are noticeably different in correspondence with the observed difference in minima depths and implied temperature difference. Preliminary mean radii (2.3 and $2.2\,R_\odot$) are slightly below the empirical mid-MS calibration of Popper (1998), but this is attributable to the system's youth.

Table 1. Curve-fitting results for *Hipparcos* photometry of V831 Cen.

Parameter	Value	Error
T_h (K)	12 100	
T_c (K)	11 500	
M_2/M_1	0.82	
L_1	0.37	0.02
L_2	0.31	
L_3	0.32	0.02
r_1 (mean)	0.39	
r_2 (mean)	0.37	
i (deg)	61.3	0.5
u_1	0.35	
u_2	0.4	
$\Delta\phi_0$ (deg)	0.4	0.3
χ^2/ν	1.03	
Δl	0.005	

Fig. 2 shows the photometric model of Table 1 matched to the data of Waelkens & Bartholdi (1982). In this case, we adopted starting geometric parameters from the *Hipparcos* fitting and then concentrated the improvements on the relative luminosities. Experiments have shown that the geometrical parameters are not so sensitive to the assigned temperatures. Table 2 lists only the broader filter (*UBVG*) relative luminosities. The *UBV* magnitudes have been scaled from Geneva to Johnson magnitudes, by converting the relative luminosities of the components in the Geneva filters, adopting the derived *Hipparcos* V-filter reference magnitude ($V = 4.55$) as definitive and using Johnson colours as reported in the SIMBAD data base to obtain U and B magnitudes. We adjusted apparent differences between Johnson and Geneva colours, using the mean wavelengths of the Johnson and Geneva system filters (cf. Budding & Demircan 2007). The G magnitude remains in the Geneva system.

The results show the expected smallness in the $B - V$ difference for the two stars of the eclipsing system, compared with the $U - B$ colours, consistent with Balmer decrement effects for late B-type stars. The third light appears relatively strong in B and rises significantly towards the G. Later analysis will show that the lower mass of V831 Cen B implies that its relative light would not exceed that of V831 Cen b: the scale of the 'third light' in V and G then indicates that light from V831 Cen C is also included in this photometry. The difference of 0.7 V mag between V831 Cen ab and V831 Cen B estimated by Worley & Douglass (1996) is consistent with the relative magnitudes of Table 2. The derived $B - V$ and $U - B$ colours of V831 Cen a and b suggest somewhat higher temperatures than those initially assigned from the types and combined colours (finally adopted values are given in Table 8). The mean phase shift of 21°.8 for the Waelkens & Bartholdi light curves (Fig. 2) together with the *Hipparcos* light-curve epoch allows the mean linear ephemeris to be better written as

$$\mathrm{Min\,I} = 2448\,500.297 + 0.642\,5251\,E, \qquad (2)$$

representing, approximately, the last 25 yr.

3 SPECTROSCOPY

The spectroscopic data of this paper were taken with the High Efficiency and Resolution Canterbury University Large Échelle

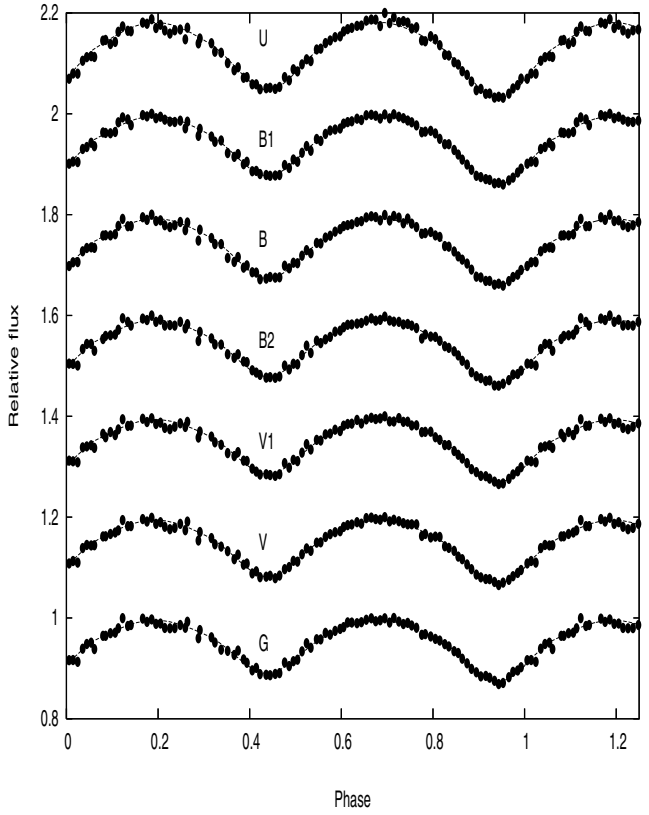

Figure 2. Light-curve fittings, derived from the geometrical elements of the *Hipparcos* data solution (Table 1) applied to the Geneva U, $B1$, B, $B2$, $V1$, V, G photometry of V831 Cen, as discussed by Waelkens & Bartholdi (1982). The relative fluxes are shown against phase with each curve vertically displaced by a linear displacement of 0.2. The greater amplitude of the light variation towards the shorter wavelengths is apparent, although the relative depths of the two minima do not change by so much. This suggests a third light from some lower temperature source or sources. There is also a conspicuous horizontal shift following from usage of the old ephemeris to calculate the phases.

Table 2. Magnitudes of stars in the V831 Cen (AB) system.

	U	B	V	G	Err.
m_a	4.973	5.525	5.640	5.663	0.02
m_b	5.235	5.715	5.836	5.932	0.03
m_3	5.793	5.764	5.761	5.684	0.03

Spectrograph (HERCULES) of the Department of Physics and Astronomy, University of Canterbury (cf. Hearnshaw et al. 2002). This was used with the 1 m McLellan telescope at the Mt John University Observatory (MJUO), near Lake Tekapo (∼43°59′S, 174°27′E). Further details are given in Paper I. 27 spectra were taken on 2006 May 19 and 20, in fairly clear conditions (occasional clouds). The 50 μm optical fibre was used, enabling a resolution of approximately 70 000. The average exposure times were about 200 s. The CCD camera was in position 2, and initial data acquisition and reduction were performed with on-site facilities including the HRSP software package (Skuljan & Wright 2007).

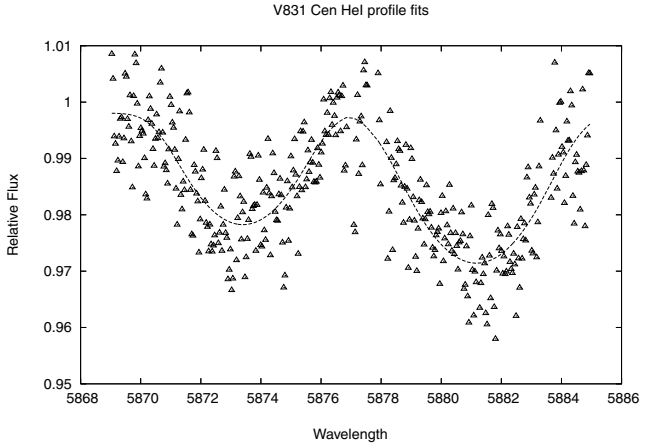

Figure 3. Results of profile fitting to the He I 5876 lines at elongation (HJD 245 3874.8078; cf. Table 4, No 2). The secondary is on the left.

3.1 Line profiles

Identifiable spectral lines for the close binary are similar to those listed in Paper I, but the relative effects of proximity in broadening out the profiles and enhancing noise or contamination are much greater for V831 Cen ab. We have concentrated on the He I 5876 feature for careful measurements of radial velocities (rvs), although the He I 6678 lines are sometimes measurable (particularly the primary). The He I lines at 5048 and 4713 tend to spread over the edge of orders and are unsuitable for clear results. Other possibilities among the lines listed in Paper I become too shallow when rotationally broadened to several angstroms, but rotational effects are determinable for the 5876 lines. The procedure followed to analyse rotational effects was given in Paper I, and the results are discussed in the next subsection.

Work with the close binary's lines is also compromised by the spectrum of the third star, which, contrary to initial expectation, produces a large number of features, having their own separate rv and (relatively small) line-broadening characteristics. This is discussed in Section 3.4, with data presented in Table 7.

3.2 Rotational velocities

We have fitted the helium line profiles of V831 Cen at elongation phases. Typical results are shown in Fig. 3 with the parameters listed in Table 3.

The meanings of the parameters in Table 3 were explained in Paper I: the parameter r, measuring the projected rotational velocity $v \sin i$, yields values of 194 and 170 km s^{-1} for primary and secondary, respectively, having taken into account the inclination 61°.3. These values are close to those of corotation, following from the derived systemic rotation speed of 480.1 km s^{-1} and the radii from Table 8, which would yield corotation values of 188 and 177 km s^{-1}, respectively. Error estimates for these speeds can be put at 4 km s^{-1}. Stars in an arrangement such as V831 Cen ab should synchronize within ∼1 Myr (cf. Vaz, Andersen & Claret 2007).

A number of lines in the third spectrum (Section 3.4) are sufficiently well defined to permit profile fitting. The average results for the Mg I lines at 5168, 5173 and 5184 Å give 34.5 ± 1.6 km s^{-1} for the rotation speed, using the adopted inclination of the A-B system and assuming parallelism of rotation and orbital motion planes ($i_{AB} = 62°.2$, according to Table 5). Results are listed in Table 3 and shown in Fig. 4.

Table 3. Profile-fitting parameters for the He I 5875 lines at HJD 245 3874.8078. (Note that the table lists vacuum mean wavelengths.)

Parameter	Value	Error
V831 Cen ab, He I 5875		
Primary		
I_c	0.998	0.001
I_d	0.0177	0.0006
λ_m	5881.175	0.072
r	3.340	0.062
s	0.2	
χ^2/ν, Δl	0.92	0.007
Secondary		
I_c	0.998	0.001
I_d	0.0177	0.0006
λ_m	5873.401	0.076
r	2.920	0.062
s	0.2	
χ^2/ν, Δl	0.82	0.007
V831 Cen B, Mg I 5184		
I_c	0.951	0.005
I_d	0.049	0.015
λ_m	5185.54	0.023
r	0.53	0.02
s	0.85	0.04
χ^2/ν, Δl	1.36	0.005

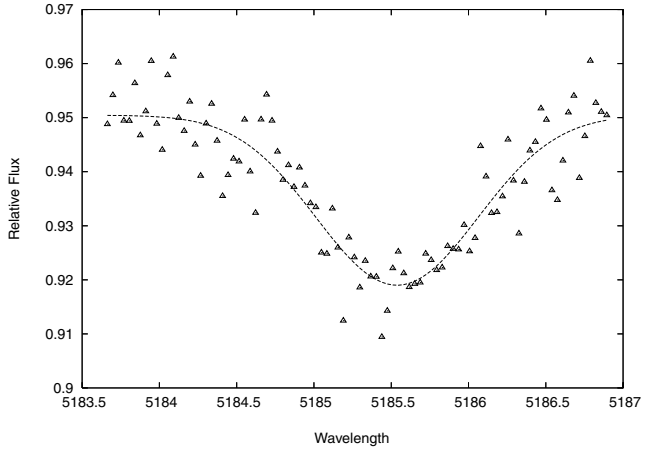

Figure 4. Results of profile fitting to selected third spectrum Mg I lines at 5184 Å. Similar results are found for the 5168 and 5173 components. The wavelengths shown are vacuum.

3.3 Radial velocities

The mean wavelengths derived from profile fitting to the He I 5876 lines allow rvs to be found, using the Doppler displacement principle, by comparison of these measured wavelengths with their rest values. The close proximity of the components, coupled with large inherent broadening, rendered the hydrogen lines of no practical value (see below). The listed dates and velocities have been corrected to heliocentric values as in Paper I (with the use of HRSP and IRAF data reduction facilities). The errors of mean line centre positions are estimated (from internal agreements of measures) at about 3.0 km s^{-1} (≈0.5 per cent of their mean widths). The full schedule of timings and rv measures is given in Table 4.

Table 4. RV data for V831 Cen ab. Individual measures have a precision of ∼3.0 km s^{-1}.

No	No HJD 245 0000 (d)	RV1 (km s^{-1})	RV2 (km s^{-1})
1	3874.7827	175.5	−181.5
2	3874.8078	189.3	−206.5
3	3874.8285	204.6	−198.9
4	3874.8314	199.5	−208.6
5	3874.8519	209.2	−208.5
6	3874.8560	205.6	−207.5
7	3870.8835	192.8	−203.5
8	3874.8881	184.1	−192.3
9	3874.9222	–	–
10	3874.9253	–	–
11	3874.9695	–	–
12	3874.9726	–	–
13	3874.9912	13.4	13.4
14	3875.0181	–	–
15	3875.0316	–	–
16	3875.0693	–126.2	174.7
17	3875.0736	–127.7	192.6
18	3875.1190	–161.5	240.4
19	3875.1775	–168.7	230.6
20	3875.1825	–164.1	242.5
21	3875.2459	−106.9	204.7
22	3875.9942	–	–
23	3876.0029	63.7	−65.3
24	3876.0241	108.4	−106.6
25	3876.0602	154.6	−188.2
26	3876.0645	164.8	−194.4
27	3876.1043	180.8	−195.5

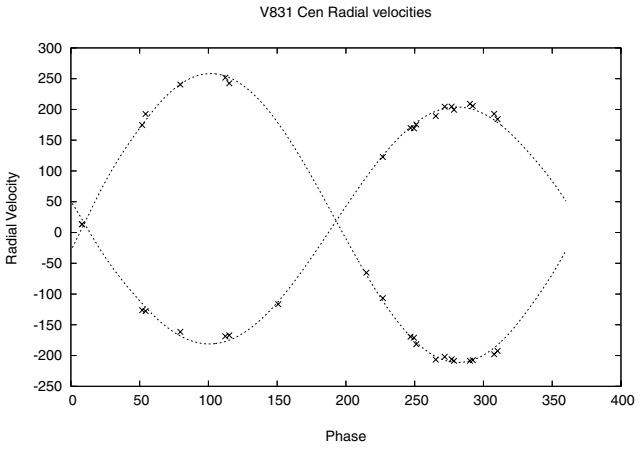

Figure 5. Measured rvs are plotted against a fitting function that takes into account both proximity and eclipse effects. The primary star approaches (more negative rvs relative to the centre of mass) after phase zero. The inclination is too low to make the Rossiter effect noticeable.

We have introduced the same fitting model for the rv variation, which includes regular proximity effects, as in Paper I. The results of applying this program to the observed rvs are shown in Fig. 5 and the corresponding parameters are given in Table 8.

3.4 Third spectrum

Apart from the close binary, the recorded spectra show the presence of V831 Cen B, for which 161 attributed line features are presented

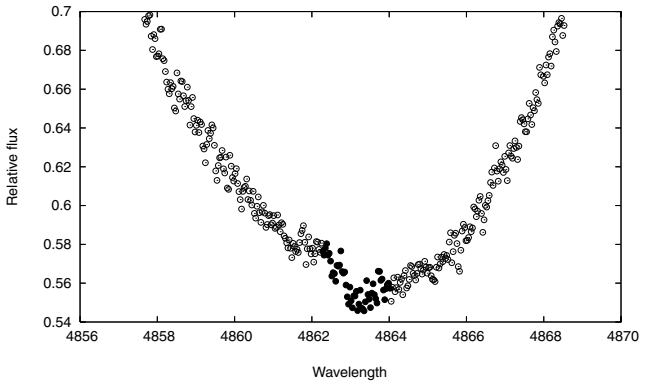

Figure 6. The central part of the combined Hβ profile at elongation (as Fig. 3). The intrusive, somewhat redshifted feature at the centre (marked with full circles) is taken to be the third star's contribution.

in Table 7. Identifications for 149 of these lines come from the revised Identification List of Lines in Stellar Spectra (ILLSS; Coluzzi 1993; Coluzzi 1999), but there are several distinct line features that have not been identified. Some of these may be complex blends. The Hβ blend is shown in Fig. 6.

Although a number of the ILLSS identifications point to cooler giant atmospheres (see the comments to Table 7), some are also seen as likely for earlier type stars. From the photometric, as well as other, evidence to be discussed later, a cool giant option for the third star seems highly unlikely. Four – possibly five – rare earth elements are among the identifications together with significant indications of chromium and manganese, which point to an Ap or perhaps Bp star (cf. e.g. Rice 1998).

In considering this information on the third spectrum, we should keep in mind the proportionately large scale of noise. To some extent this is evident in Fig. 4, but Table 7 lists the Mg I features as having relatively large equivalent widths (EW) of ∼30–40 mÅ. The EW values in this table were derived using the IRAF tool 'SPLOT'. Exposed orders are typically 10 pixels across, where one pixel width accounts for about 1/40 Å and registers a count of typically ∼3000. A feature wider than 0.25 Å with an EW of ∼1 mÅ should thus correspond to a continuum count deficit of about 300 or comparable to the probable error of the measurement. The average half-width of features listed in Table 7, excluding very broad or blended lines, is about 0.43 Å as measured with SPLOT. The third star accounts for only about 20 per cent of the combined light: the Eu II (4627) line, listed with an EW of 9 mÅ, would actually correspond to an EW of 45 mÅ on V831 Cen B, comparable to typical values for an Ap star (e.g. Aslanov et al. 1973). Features with EW greater than ∼3 mÅ in Table 7 can therefore be taken seriously, though the appreciable scatter in individual Doppler shifts is understandable. The average shift from the full list of 149 identified absorption lines is $+28.8\,\mathrm{km\,s^{-1}}$, but with the large s.d. of $8.1\,\mathrm{km\,s^{-1}}$. Removing outliers, lines of low weight and blends, we find the same $+28.8\,\mathrm{km\,s^{-1}}$ from 122 lines, but with the s.d. reduced to $6.1\,\mathrm{km\,s^{-1}}$. The Mg I line fittings give a recession of $+27.6\,\mathrm{km\,s^{-1}}$ with an s.d. of $2.1\,\mathrm{km\,s^{-1}}$. It is very significant that this rv excess of the third star with respect to the mean space velocity of the close pair is confirmed by the astrometry discussed in the next section.

Another point to note about the identifications in Table 7 is that the echelle orders covered by this camera do not give continuous spectral coverage. There is thus a significant number of expectable lines, of a Ba II multiplet for example, in the inter-order gaps. Table 7 should thus be seen more as a pointer to chemical peculiarity than as a definite proof of a particular type.

4 ASTROMETRY

It is becoming increasingly possible, in the era of higher resolution astronomy, to consider the complete geometric configuration of stellar systems. This is likely to become a common feature of close binaries that are in young and relatively near star groupings, because of the common presence of components at angular distance scales in the order of tens of mas. The main additional outcomes from such studies are nodal angles and inclinations as well as, from Kepler's laws, masses of the stars.

Finsen (1964) (cf. also Worley & Heintz 1983) provided a set of elements for the See 170 system, taken to be three late B-type stars, two in the almost-contact configuration V831 Cen (ab) and the third (B) in a 27.00 yr period orbit. Mason et al. (2006) gave more recent astrometric data on the A-B binary, which can be analysed along previously given lines; thus, for the standard coordinates of the relative orbit,

$$X = \frac{a(1-e^2)}{1+e\cos\nu}[\cos(\nu+\omega)\sin\Omega - \sin(\nu+\omega)\cos\Omega\cos i], \quad (3)$$

$$Y = \frac{a(1-e^2)}{1+e\cos\nu}[\cos(\nu+\omega)\cos\Omega + \sin(\nu+\omega)\sin\Omega\cos i]. \quad (4)$$

These equations can be related to the differential positional measurements of the binary ρ and θ, since

$$-\rho\sin\theta = X \quad (5)$$

and

$$\rho\cos\theta = Y; \quad (6)$$

that is, the measures are directly related to the five orbital parameters a, e, ω, i and Ω. To fix the configuration at a given time, we need, as well as the period P, the epoch of periastron passage T_0. A provisional value for T_0 could be deduced from the information given by Mason et al. (2006) as 1887.1. There are thus seven unknown parameters altogether for an optimization of the astrometric orbital model. We have calculated χ^2 from a nested subroutine within an ILOT program environment (cf. Budding & Demircan 2007), using the elements of Finsen as starting values. Although there is insufficient information in the data to permit a well-determined seven-parameter set, good-fitting values (in the χ^2 sense) are found close to the Finsen set. The adopted result is shown in Fig. 7, and the corresponding parameters are listed in Table 5, together with indicative error estimates. It is interesting that a good-fitting inclination for the A-B system appears close to that of the close binary. Within the errors of measurement, we could say that the V831 Cen ab and See 170 systems are consistent with coplanar orbits.

The semimajor axis, at the *Hipparcos* distance of 106 pc, implies a physical separation of 19.1 au for See 170AB. Kepler's law will then yield $9.4\,\mathrm{M}_\odot$ for the total mass of the system. The photometric + spectroscopic solutions suggested masses of 4.1 and $3.3\,\mathrm{M}_\odot$ for the close binary (A), so the total mass of the A-B system is in agreement with this if the third star is an $\sim 2.0\,\mathrm{M}_\odot$ near-MS object. A larger distance to the system (see below) will increase the mass of the third component.

The rv excess of the third star, according to the orbit model of Table 5, corresponds, at the observed phase of about 0.381, to about $12.0\,\mathrm{km\,s^{-1}}$ in recession (using formula 9.8 in Budding & Demircan 2007). The previously mentioned spectrographic rv of

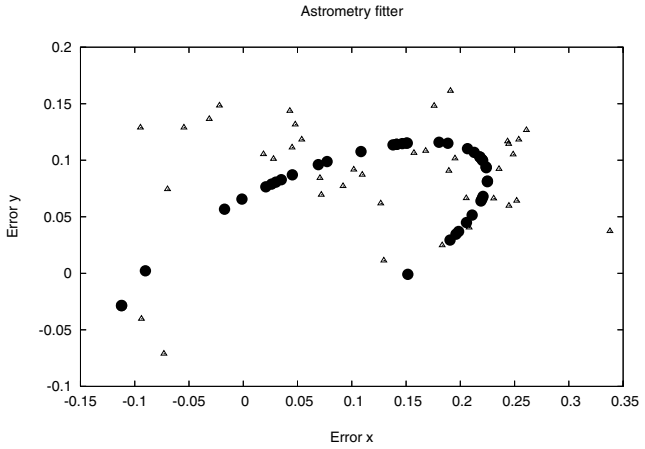

Figure 7. Fitting to the astrometric orbit of See 170. The open triangles represent the observations of separation and position angle. Corresponding orbital positions are indicated by the sequence of full circles.

Table 5. Astrometric elements for See 170.

Parameter	Value	Error
P (yr)	27.2	0.4
a (mas)	180	20
i (deg)	62.2	2.0
Ω (deg)	−104	5
T_0 (yr)	1887.2	0.6
e	0.48	0.1
ω (deg)	219	5
$m_1 + m_2 + m_3(\mathrm{M}_\odot)$	9.4	
Fitting stat.	$\chi^2/\nu = 1.3$	$\Delta s = 50$ (mas)

$27.6 \pm 2.1\,\mathrm{km\,s^{-1}}$ is then an acceptable $10.2\,\mathrm{km\,s^{-1}}$ greater than the systemic velocity ($17.4\,\mathrm{km\,s^{-1}}$) of the close binary.

In addition to See 170, Mason et al. also provided observations for I424 (the AB-C system). These trace out an almost linear short trend when plotted, so it seems clear that this limited coverage of the orbit could not be used to establish its full set of parameters. The data cover only about 90 yr of a period that must be on the order of a thousand years. Given the low rate of change of the true anomaly ($\sim 20^\circ$), we can expect that the AB-C orbit is quite eccentric: from the Equation of the Centre $(\nu - M) \sim (2e - e^3/4)\sin M$, e could be as much as 0.5.

In order to make progress, we posit coplanarity of the AB-C system so that i can be retained from the A-B orbit. The positional trend's location, orientation on the sky, length and slight curvature then enable derivations of feasible values for the parameters a, ω, Ω and T_0, given that P can be estimated as $\sim$2000 yr, if V831 Cen C is a main-sequence star of about $1.5\,\mathrm{M}_\odot$. The latter follows from the magnitude difference AB-C of about 2.9 mag in V. We show the corresponding set of parameters in Table 6, and the resulting orbit is shown in Fig. 8.

5 ABSOLUTE PARAMETERS

SIMBAD gives the reference V magnitude for V831 Cen from *Hipparcos* as 4.583. In forming the light curve in Fig. 1 we used the *Hipparcos* photometry and (following the procedures given in the CURVEFIT manual; Rhodes, 2008) selected the brightest point from which to convert magnitude differences to relative flux values, and thence derive the mean out-of-eclipse 'unit of light' that corrects for

Table 6. Astrometric curve fitting for the wide binary I424.

Parameter	Value	Error
P (yr)	∼2000	
a (mas)	3.2	0.1
e	0.5	
ω (deg)	80	
i (deg)	68	
Ω (deg)	−85	
T_0 (yr)	1084.5	3.0
Error meas.	$\chi^2/\nu = 0.94$	$\Delta s = 0.15$ (as)

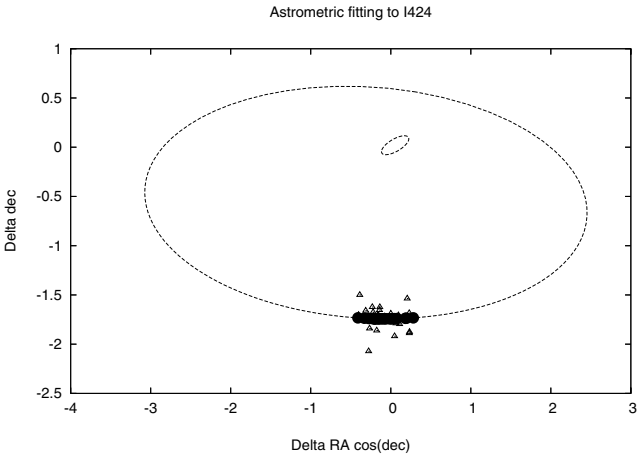

Figure 8. Fitting to the observed small segment of the orbit of I424. Open triangles and full circles are observations and predicted positions as before. The calculated full orbits of I424 and See 170 are shown. V831 Cen ab is located at the coordinate origin.

the proximity effects calculated in the fitting program. This results in $V = 4.55$, although here it should be noted (as in SIMBAD) that this value includes the additional contribution of V831 Cen B and probably also V831 Cen C.

The magnitudes in Table 2, coupled with the adopted temperatures and radii, using the formula for the parallax π in terms of radius R, magnitude V and surface flux F'_V (Budding & Demircan 2007)

$$\log \pi = 7.454 - \log R - 0.2V - 2F'_V, \tag{7}$$

yield distances of 121 and 126 pc for V831 Cen a and b, respectively; rather they are greater than those of *Hipparcos*, although it is a recognized fact that the latter was not a good determination due to the complications of source multiplicity. The compromise distance of 110 pc is thus adopted in Table 8.

6 DISCUSSION

Most stars in the Galaxy are thought to have originated in OB associations: large stellar groups made conspicuous by the relatively bright and massive young stars of early spectral type within them. Detailed knowledge of the formation and properties of such structures should thus contribute to a broader understanding of galactic structure and evolution. But this kind of knowledge still tends to be largely summary in character, even for the nearest OB associations. This is partly because their large angular extent renders the identification of their members not obvious (cf. Preibisch & Zinnecker 2007). Proving the membership of particular stars has sometimes

Table 7. Spectrum measures for V831 Cen B.

Measured	Reference	EW	Δλ	Species	Rem.	Measured	Reference	EW	Δλ	Species	Rem.
6519.368	?	10		?	1	5481.762	5481.17	13	0.592	Fe I	7
6515.598	6515.026	23	0.572	Cr I		5478.730	5478.48	7	0.250	Fe I	7
6514.665	?	13	?	?		5477.096	5476.57	9	0.526	Fe I	
6479.582	?	10	?	?	2	5455.982	5455.613	24	0.369	Fe I	4
6475.377	6474.61	12	0.767	Fe I		5430.199	5429.699	18	0.500	Fe I	4
6470.622	6470.25	11	0.372	Zr I		5424.458	5424.072	17	0.386	Fe I	4
6469.643	6469.12	6	0.523	Fe I		5415.781	5415.210	12	0.571	Fe I	8
6463.211	6462.566	16	0.645	Ca I	3, 4	5406.322	5405.778	5	0.544	Fe I	8
6460.689	?	59		?	5	5372.047	5371.493	21	0.554	Fe I	8
						5370.309	5369.965	19	0.344	Fe I	8
6454.528	?	23		?	2	5367.974	5367.470	9	0.504	Fe I	8
6450.284	6449.810	16	0.474	Ca I		5365.430	5364.874	15	0.556	Fe I	8
6400.704	6400.010	7	0.694	Fe I	4	5328.761	5328.534	23	0.227	Fe I	7, 8
6395.720	6395.16	5	0.560	Ca I		5324.622	5324.185	19	0.437	Fe I	8
6394.402	6393.605	8	0.797	Fe I	4	5317.142	5316.609	8	0.533	Fe I	4
6193.462	6192.96	9	0.502	Zr I		5276.371	5275.994	8	0.378	Fe II	4, 7
6192.072	6191.562	4	0.510	Fe I		5275.346	5274.99	3	0.356	Cr II	
6169.744	6169.307	3	0.437	Ca I	6	5273.762	5273.379	5	0.383	Fe I	7, 9a
6122.900	6122.219	5	0.681	Ca I	4	5262.290	5261.706	13	0.584	Ca I	4
6106.871	6106.19	4	0.681	Gd II	9	5257.535	5256.89	7	0.645	Fe II	
6104.674	?	2		?		5255.394	5254.956	12	0.438	Fe I	8
6103.241	6102.722	10	0.519	Ca I	4	5233.252	5232.946	8	0.306	Fe I	7, 8
6066.123	6065.81	4	0.313	Fe I		5230.209	5229.857	10	0.352	Fe I	8
6046.693	6046.36	8	0.333	O I	4, 6	5227.309	5226.868	17	0.441	Fe I	8
5993.381	5992.65	3	0.731	Fe I		5220.883	5220.297	5	0.586	Gd II	9
5991.913	5991.58	8	0.333	Fe I		5217.887	5217.395	9	0.492	Fe I	
5976.98	5976.18	5	0.800	Fe I		5215.773	5215.185	6	0.588	Fe I	
5971.34	?	8		?		5208.930	5208.436	22	0.494	Cr I	8
5970.20	5969.55	6	0.65	Fe I		5206.289	5206.039	16	0.250	Cr I	8
5968.094	5967.77	8	0.324	V II		5184.047	5183.604	42	0.443	Mg I	4
5942.512	5941.755	12	0.757	Ti I		5173.193	5172.684	31	0.509	Mg I	4
5938.072	5937.806	8	0.266	Ti I		5169.558	5169.030	5	0.528	Fe II	4
5930.794	5930.173	4	0.621	Fe I		5167.854	5167.322	29	0.532	Mg I	4
5924.036	?	12		?	7	5139.868	5139.260	9	0.608	Fe I	8
5922.525	5922.112	10	0.413	Ti I	8	5137.733	5137.388	7	0.345	Fe I	8
5912.916	?	7		?		5127.945	5127.363	10	0.582	Fe I	8
5911.941	5911.450	6	0.491	Gd II	9	5124.032	5123.723	7	0.309	Fe I	8
5910.448	5909.990	7	0.458	Fe I		5049.059	5048.454	11	0.605	Fe I	
5862.798	5862.375	5	0.423	Fe I	8	5022.566	5022.244	5	0.322	Fe I	7, 8
5858.034	5857.454	10	0.580	Ca I	8	5020.500	5020.028	6	0.472	Ti I	8
5854.462	5853.675	5	0.787	Ba II	4	5018.832	5018.434	18	0.398	Fe II	4
5817.70	5817.30	9	0.40	V I	7	4991.481	4991.067	9	0.414	Ti I	8
5788.75	5787.99	4	0.76	Cr I	8	4957.885	4957.302	23	0.583	Ba II	
5785.58	5785.002	4	0.578	Cr I	8	4953.851	4953.370	6	0.481	Ti I	7
5737.98	5737.04	2	0.94?	V I	8	4934.600	4934.086	25	0.514	Ba II	4
5732.56	5731.771	5	0.789	Fe I	7	4914.168	4913.616	12	0.552	Ti I	
5729.65	5729.203	10	0.447	Cr I		4912.732	?	8		?	
5701.903	5701.35	3	0.553	Gd I		4908.415	?	2		?	
5700.829	5700.14	2	0.689	Sc I		4890.276	4889.730	11	0.546	Cr I	
5698.746	5698.37	3	0.376	Fe I	8	4876.902	4876.190	29	0.712	Fe I	
5697.104	5696.63	2	0.474	S I		4861.937	4861.332	32	0.605	H_β	10
5695.50	5694.73	8	0.77	Cr I	7	4823.923	4823.516	7	0.407	Mn I	4
5694.149	?		?	3		4783.793	4783.420	4	0.373	Mn I	8
5692.37	5691.69	2	0.68	Fe I		4779.787	4779.444	15	0.343	Fe I	
5688.62	5688.205	3	0.45	Na I	6	4767.555	4766.87	5	0.685	Fe I	
5687.21	5686.532	3	0.678	Fe I	7	4747.657	4747.000	12	0.657	Cr I	7
5644.747	5644.350	4	0.397	Fe I		4745.641	4745.308	4	0.333	Cr I	8
5642.358	5641.880	3	0.478	Ni I		4699.062	4698.615	4	0.447	Cr I	8
5638.663	5638.266	3	0.397	Fe I		4673.481	4672.83	4	0.651	Fe I	7
5637.813	5637.121	3	0.692	Ni I		4667.481	4666.75	9	0.731	Fe II	4
5637.048	5636.708	3	0.340	Fe I		4665.857	4665.24	4	0.617	Fe I	
5634.362	5633.95	4	0.412	Fe I		4636.121	4635.62	11	0.501	Fe I	7
5624.897	5624.549	3	0.348	Fe I	8	4627.673	4627.220	11	0.453	Eu I	9

Table 7 – *continued*

Measured	Reference	EW	Δλ	Species	Rem.	Measured	Reference	EW	Δλ	Species	Rem.
5621.016	5620.527	8	0.489	Fe I	7	4596.392	4595.951	8	0.441	Ni I	
5617.866	5617.14	2	0.726	Fe I		4595.089	4594.510	15	0.579	Ti I	
5616.071	5615.652	9	0.419	Fe I	8	4591.967	4591.394	6	0.573	Cr I	
5614.804	5614.29	6	0.224	Fe I	7	4584.394	4583.829	10	0.565	Fe II	4
5587.067	5586.763	6	0.304	Fe I	8	4581.917	4581.402	17	0.515	Ca I	4
5582.620	5581.971	9	0.649	Ca I	4	4577.617	4577.173	6	0.444	V I	8
5580.036	5579.34	8	0.696	Fe I		4572.498	4571.971	6	0.527	Ti II	4
5573.404	5572.849	21	0.555	Fe I	7, 8	4564.010	4563.761	13	0.249	Ti II	4
5570.080	5569.625	7	0.455	Fe I	7, 8	4560.760	4560.28	7	0.480	Ce II	7
5566.191	5565.697	8	0.494	Fe I		4556.481	4555.89	5	0.591	Fe II	4
5562.942	5562.12	5	0.822	Fe I	7	4554.447	4553.949	11	0.498	Cr I	7
5560.149	5559.64	2	0.509	Fe I		4550.091	4549.467	5	0.624	Fe II	4
5538.877	5538.54	5	0.337	Fe I	7	4538.406	4537.952	9	0.454	Sm II	9
5535.617	5534.86	3	0.757	Fe II	4	4536.211	4535.747	8	0.464	Ti I	6
5528.869	5528.399	28	0.479	Mg I	4	4525.290	4524.744	9	0.546	Sn I	
5522.934	5522.46	6	0.474	Fe I		4520.429	4520.225	12	0.204?	Fe II	4, 9a
5513.189	5512.529	5	0.660	Ti I	8	4509.288	4508.52	7	0.768	Ti I	9a
5509.219	5508.880	6	0.339	Cr I		4508.561	4508.26	6	0.301	Fe II	4

Note. The columns are mostly self-explanatory. EW are listed in units of mÅ of the *combined* local continuum. Remarks (Rem) as follows, 1: a number of distinct features could not be identified, though apparently similar to identified ones; 2: wavelength consistent with N III, but formation unclear; 3: distorted by nearby emission; 4: associated with hotter, low *g* sources; 5: emission feature; 6: close doublet blend; 7: blend; 8: cooler, low *g* source expected; 9: rare earth element; 9a: possible blend with rare Earth; 10: narrow feature in core of the broad blend from the close binary. Data from which this table was composed can be made available to any interested specialist.

Table 8. Adopted absolute parameters for the V831 (close) system. Formal errors are indicated by the parenthesized numbers affecting the latter digits of the solution numbers (see also Section 3.3).

Parameter	Value
Period (d)	0.642 5251
Epoch (HJD)	244 8500.297
V_0, $(B-V)_0$, $(U-B)_0$	4.532, −0.08, −0.38
$E(B-V)$	0.04
A_{12} ($R_\odot$)	6.09(2)
$K_{1,2}$ (km s^{-1})	189.8 (1.7), 231.3(2.0)
V_γ (km s^{-1})	17.4(2.2)
$M_{1,2}$ ($M_\odot$)	4.08(7), 3.35(6)
$R_{1,2}$ ($R_\odot$)	2.38(3), 2.25(3)
$T_{1,2}$	13 000 (300), 11 800 (300)
Distance (pc)	110 (10)
Age (Myr)	18 (3)

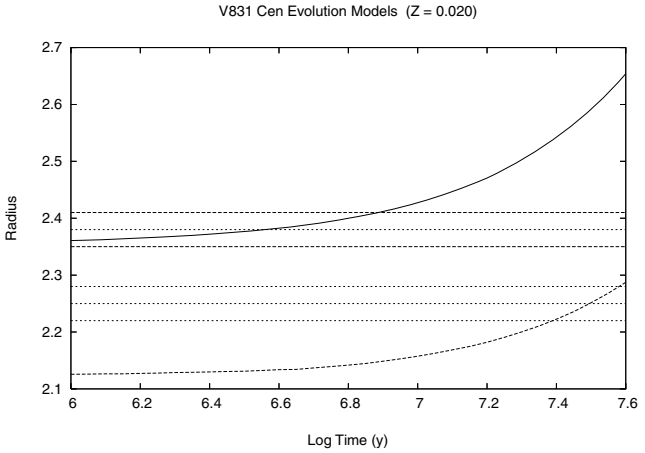

Figure 9. The growth of mean radii (V831 Cen a and b) with age is shown according to the Padova models for $Z = 0.02$. As with U Oph, a significant disparity between ages of primary and secondary can be seen, although the mean age is in agreement with other circumstantial evidence.

been a protracted task. Considerable progress was made in the wake of the *Hipparcos* survey (de Zeeuw et al. 1999).

The SCOB association is the nearest example of its kind to the Sun. It contains hundreds of B stars that tend to concentrate in the three subgroups of Upper Scorpius, Upper Centaurus Lupus and LCC. V831 Cen is in this latter region (Nitschelm 2003), which is thought to be intermediate in age between the other two. The SCOB association lies within a large bubble of hot gas that is indicated by signs of stellar winds from the many massive stars in the association as well as various supernova explosions that happened during the last several million years. These effects testify to the relative youth of the SCOB association. It is thus of interest to check general parameters of the SCOB association against detailed studies of individual member stars where possible.

We have used the Padova data base of stellar evolution data[1] that incorporates the calculations of Girardi et al. (2000) and Marigo et al. (2008) to determine the growth of radii of the components of V831 Cen a and b. Results are shown in Fig. 9. In constructing these plots, we set the metallicity $Z = 0.02$. It can be seen from Fig. 9 that the primary component has attained measured radius by ∼5 Myr, while the measured radius of the secondary component is not reached (by normal single star evolution) until ∼30 Myr. An oversized status of the secondary was found also for U Oph, and this point may require further (future) consideration. However, we may also note, from Section 3.2, that the derived rotational

[1] pleiadi.pd.astro.it/#data10

velocities, if corotational, would imply a larger primary ($2.46\,R_\odot$) and smaller secondary ($2.16\,R_\odot$), resulting in a better agreement for the individual ages with about the same average. This may then comment on the photometric determinacy discussed in Section 2. For the present, we find reasonable agreement between the average age of the V831 Cen stars determined from their mean radii and the results of Mamajek, Meyer & Liebert (2002), who found that, depending on the choice of published evolutionary tracks, mean ages of LCC stars range between 17 and 23 Myr.

At the adopted distance of 110 pc, the derived mass of V831 Cen B turns out as $\sim 2.5\,M_\odot$, and its bolometric and V luminosities should then be $\approx$18 and 22 per cent, respectively, that of the A-B binary. This is still less than that of the third light contribution in Table 1. An implication is then that the third light may also contain that of V831 Cen C, which would be a further $\approx$5 per cent in V.

The overall picture of V831 Cen is then of a young, almost contact, but still unevolved central massive $\sim 4.1 + 3.4\,M_\odot$ eclipsing binary system with a chemically peculiar third $\sim 2.5\,M_\odot$ star at about 20 au separation, a fourth star of perhaps $\sim 1.5\,M_\odot$ at $\sim$350 au and at least one more lower mass companion still further out. This hierarchical structure has come into being over the last $\sim$20 Myr, in the wake of star formation processes in the Lower Centaurus Crux region of the Sco-Cen OB2 association within the Gould Belt's megastructure. Our results have a general coherence and improved young star parametrization, but V831 Cen still offers interesting challenges about its physical details, concerning the properties of the (assumed) Ap component, for example. It will surely repay continued observations and analysis.

ACKNOWLEDGMENTS

The authors are very appreciative of the provision of the seven-colour Geneva photometry by Dr G. Burki of the University of Geneva, intermediated by Dr C. Waelkens of the Leuven Observatory. We greatly appreciate the financial support of the Turkish Science Research Council (TUBITAK) in partial support of this programme, as well as the Carter National Observatory of New Zealand. The Observatory's former Manager (J. Marchand) and former Senior Astronomer (B. Carter) provided well-received hospitality and encouragement.

Generous allocations of time on the 1 m McLennnan Telescope and HERCULES at the Mt John University Observatory were made available through its TAC and supported by its Director, Professor J. Hearnshaw. Useful assistance at the telescope were provided by the MJUO management (A. Gilmore and P. Kilmartin) as well as (particularly) Duncan Wright and other students and staff of the Department of Physics and Astronomy, University of Canterbury, Christchurch.

V. and H. Bakış, D. Doğru and B. Özkardeş of the Department of Physics, 18th March University of Çanakkale, Turkey, have given appreciated assistance with practicalities of this programme. We also acknowledge the constructive comments of Professors M.-E. Özel and Z. Eker of that department, and especially Dr H. Hensberge, Royal Observatory of Belgium.

REFERENCES

Aslanov I. A., Heildebrandt G., Khokhlova V. L., Schöneich W., 1973, Ap&SS, 21, 477
Blaauw A., 1964, in Kerr F. J., ed., Proc. IAU Symp. 20, The Galaxy and The Magellanic Clouds. Australian Academy of Sciences, Canberra
Budding E., 2009, in Zhang S. N., Li Y., Yu Q. J., eds, 10th Asian Pacific Regional Meeting of IAU, Kunming, China. National Obs. China Press, in press
Budding E., Demircan O., 2007, An Introduction to Astronomical Photometry. Cambridge Univ. Press, Cambridge
Budding E., İnlek G., Demircan O., 2009, MNRAS, 393, 501 (Paper I)
Coluzzi R., 1993, Bull. Inf. Centre Donnees Stellaires, 43, 7
Coluzzi R., 1999, VizieR Online Data Catalog, VI 71A
de Zeeuw P. T., Hoogerwerf R., de Bruijne J. H. J., 1999, AJ, 117, 354
ESA, 1997, The *Hipparcos* and Tycho Catalogues, ESA SP-1200. ESA, Noordwijk
Finsen W. S., 1964, AJ, 69, 319
Girardi L., Bressan A., Bertelli G., Chiosi C., 2000, A&AS, 141, 371
Hearnshaw J. B., Barnes S. I., Kershaw G. M., Frost N., Graham G., Ritchie R., Nankivell G. R., 2002, Exp. Astron., 13, 59
Kopal Z., 1959, Close Binary Systems. Chapman & Hall, London
Mamajek E. E., Meyer M. R., Liebert J. W., 2002, A&AS, 34, 762
Marigo P., Girardi L., Bressan A., Groenewegen M. A. T., Silva L., 2008, A&A, 482, 833
Mason B. D., Hartkopf W. I., Wycoff G. L., Holdenried E. R., 2006, AJ, 132, 2219
Nitschelm C., 2003, in Lepine J., Gregorio-Hetem J., eds, Astrophysics and Space Science Library Vol. 299, Open Issues in Local Star Formation. Contents of the CD-ROM: Poster Contributions. Kluwer, Dordrecht, p. 16
Nitschelm C., 2004, in Hilditch R. W., Hensberge H., Pavlovski K., eds, ASP Conf. Ser. Vol. 318, Spectroscopically and Spatially Resolving the Components of the Close Binary Stars. Astron. Soc. Pac., San Francisco, p. 291
Popper D. M., 1998, PASP, 110, 919
Preibisch T., Zinnecker H., 2007, in Elmegreen B. G., Palous J., eds, Proc. IAU Symp. 237, Triggered Star Formation in a Turbulent ISM. Kluwer, Dordrecht, p. 270
Rhodes M. D., 2008, CurveFit manual, obtainable from http://home.comcast.net/ michael.rhodes/
Rice J. B., 1998, A&A, 199, 299
Skuljan J., Wright D., 2007, HERCULES Reduction Software Package (HRSP), version 3, Univ. Canterbury, New Zealand
Vaz L. P. R., Andersen J., Claret A., 2007, A&A, 469, 285
Waelkens C., Bartholdi P., 1982, A&A, 108, 51
Worley C. E., 1978, Publ. USNO, 24, pt6
Worley C. E., Heintz W. A., 1983, Publ. USNO, 24, pt7
Worley C. E., Douglass G. G., 1996, VizieR Online Data Catalog, I/237

This paper has been typeset from a TEX/LATEX file prepared by the author.